73rd International Astronautical Congress (IAC), Paris, France, 18-25 September 2022.

IAC-22-B.2.5.8

Satellite Uplink Interference Measurements in the 437 MHz UHF Amateur Radio Band Onboard LUME-1

Gara Quintana-Diaz[a], Torbjörn Ekman[*a], Alejandro Camanzo[b], Roger Birkeland[c], José Miguel Lago Agra, Alberto González Muíño[d], Fernando Aguado Agelet[ae]

[a]*Department of Electronic Systems, Norwegian University of Science and Technology (NTNU), O.S. Bragstads plass 2b, 7034 Trondheim, Norway, torbjorn.ekman@ntnu.no*
[b]*Escola de Enxeñaría de Telecomunicación, University of Vigo, Vigo, Spain*
[c]*Department of Electronic Systems, Norwegian University of Science and Technology (NTNU), O.S. Bragstads plass 2b, 7034 Trondheim, Norway,*
[d]*Alén Space, Nigrán, Spain*
[e]*Escola de Enxeñaría de Telecomunicación, University of Vigo, Vigo, Spain*

Abstract

Satellite operators struggle to communicate with their satellites in the UHF amateur band (430–440 MHz) due to high power in-orbit interference. Statistical characterisation of the interference beyond average interference levels using in-orbit measurements is useful for the design of suitable counter measures. Some recent studies have started to investigate both the frequency and time behaviour of the interference, but more measurements are needed to cover the whole UHF amateur band. In this paper, we use the Local Mean Envelope (LME) method to analyse the time and frequency characteristics of in-orbit radio interference from the LUME-1 in the 437 MHz band. Satellite measurements were performed on TOTEM, a Software-Defined Radio (SDR), in orbit and the results were analysed on the ground. The average power spectrum and the variability of the LME for different time windows in the 437 MHz band are presented. The data analysis also includes the coefficient of variation of the LME to study the dispersion of the interference. The results are compared to measurements using the same method in the 435 MHz band. More measurements are needed for better spatial resolution. Knowledge of the time and frequency variability of the interference can indicate which mitigation techniques are required to improve satellite communication in the band.
Keywords: amateur radio band, interference statistics, in-orbit measurements, small satellite, UHF, UHF.

Acronyms/Abbreviations

AWGN	Additive White Gaussian Noise.
CV	coefficient of variation.
DFT	Discrete Fourier Transform.
ECDF	Empirical Cumulative Density Function.
ESA	European Space Agency.
IQ	In-Phase and Quadrature.
ISS	International Space Station.
ITU	International Telecommunication Union.
LME	Local Mean Envelope.
NTNU	Norwegian University of Science and Technology.
SDR	Software-Defined Radio.
TU Berlin	Technische Universität Berlin.
UVigo	University of Vigo.

1. Introduction

The 400–500 MHz UHF band encompasses several bands used for satellite communications, such as the 401 – 403 MHz Earth Exploration Satellite Service (EESS) or the amateur band from 435 to 438 MHz. The amateur radio band has been a popular choice for university small satellites missions [1]. However, not all such missions follow the correct procedure and apply for frequencies to the International Telecommunication Union (ITU) [2]. This situation, combined with the operations challenges experienced by past and current satellite missions [3, 4, 5, 6], motivate in-orbit radio measurements to better map the interference environment.

Spectrum monitoring applications and interference analysis has been promoted by the European Space Agency (ESA) in different projects [7, 8, 9, 10]. In addition, space spectrum monitoring has become a popular business case for several companies, such as Aurora Insight [11], Umbra [12], HawkEye 360 [13], Kleos Space [14] and Horizon Technologies (Amber) [15].

With a better understanding of the interference environment and the characteristics of the interference, more resilient radio systems can be designed. Since some interference sources cannot be inhibited, satellite operators need to learn how to co-exist with the interference and how satellite communication systems can be improved.

In this paper, we present new in-orbit results from measurement campaigns carried out in February and June 2022 with the LUME-1 satellite. The centre frequency is

437.28 MHz to cover the LUME-1 operations frequency [16] and the SelfieSat frequency [17]. We also compare the new 150 results with the previous measurements over the same area performed from December 2020 to June 2021 centered at 435 MHz.

The following subsection summarises the state-of-the-art of in-orbit interference measurements. In section 2, the LUME-1 satellite is introduced, the measurement algorithm applied is briefly explained and the measurement campaign is described. The results are explained and discussed in section 3. Finally, the conclusions are presented in section 4.

1.1 Related Work

The Technische Universität Berlin (TU Berlin), the University of Vigo (UVigo) and the University of Würzburg have performed spectrum after experiencing difficulties operating their satellites [4, 6, 3]. TU Berlin and UVigo encountered problems operating their satellites, TUBSAT and HumSat-D during 2013. UVigo detected strong pulsed interference. Furthermore, University of Würzburg measured high-power interference over central Europe using the UWE-3 satellite. TU Berlin continued performing interference measurements by installing an Software-Defined Radio (SDR) in the International Space Station (ISS) for spectrum monitoring in 2019 and launching the SALSAT satellite a year after.

However, most of the published results on interference measurements from small satellites in the UHF band focus on the average interference power over a certain measurement duration [6], and do not consider the time structure of the interference. Heatmaps have been a traditional way of showing the average power of interference [4, 6], but they do not show the time variability or dispersion of the interference. In this paper, both the time and frequency characteristics of the interference are analysed.

2. Material and Methods

2.1 LUME-1

The LUME-1 is a 2U satellite developed by UVigo (Spain) that was launched in a polar orbit in 2018. The mission for LUME-1 was to detect and monitor forest fires for the Fire RS European project [18]. Since the mission ended in June 2019, the satellite was available for other research. The Norwegian University of Science and Technology (NTNU) is collaborating with UVigo to use the satellite for in-orbit radio measurements. The satellite measurements are performed with the SDR and the turnstile antenna on-board LUME-1. The frequency band of the SDR is the UHF amateur radio band (435–438 MHz) and the measurements discussed in this article have been centered at 437.28 MHz. Both the uplink and the downlink throughput is limited for LUME-1. The estimated net downlink data rate is about 1 kbps, and the uplink, 200 bps both available for 5 minutes a day. The uplink is severely affected by the interference we measure in this paper. Due to these constraints, the analysis algorithm used onboard had to generate very little data and onboard processing was performed to reduce the data volume.

2.2 Analysis algorithm

To overcome the limitations of the data throughput and still analyse both the time and frequency characteristics of the interference, the Local Mean Envelope (LME) algorithm was designed [19]. The In-Phase and Quadrature (IQ) samples are acquired by the SDR and continuous Discrete Fourier Transforms (DFTs) are applied with no overlap during the measurement period. The overall mean and the average power of each frequency bin are calculated. The average power can be used to plot heatmaps. Furthermore, the local mean envelope for time windows of different lengths for every frequency bin allows the time variability analysis. The first-order stationarity window can be estimated using the coefficient of variation (CV).

2.3 Measurement campaigns

The area of interest in this paper is Europe, with a particular focus on Vigo (Spain) and Trondheim (Norway). Two measurement campaigns were performed during 13th–18th February 2022 and 25th–27th June 2022. The satellite ground tracks during measurements are shown in fig. 1. The blue tracks are the new measurements centered at 437.28 MHz (February-June 2022) and the red tracks belong to the measurements centered at 435 MHz (spring 2021) and analysed in [19]. Each circle represent one individual measurement that lasts for five seconds.

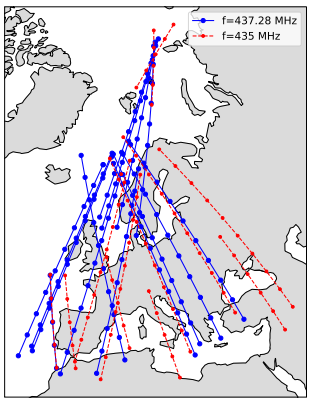

Fig. 1. Measurements tracks centered over Europe.

The configuration of the measurements is shown in table 1.

Table 1. Measurement configuration

Parameter	Value
Centre frequency (MHz)	437.28
Bandwidth (kHz)	500*
Number of frequency bins	128
Frequency resolution (kHz/bin)	4.8

*The bandwidth was configured to 200 kHz but the 3 dB bandwidth is larger [19].

3. Results and discussion

To get an overview of the frequency and time variability of the interference, the percentiles of the average power spectra and the coefficient of variation are shown in fig. 2 for both centre frequencies. The power spectra is averaged over 5 s and in every pass the individual measurements are every minute. The absolute power values have not been calibrated so the numbers shown are relative values. The CV is defined in [19] and it gives an indication of the spread in magnitude.

The 50% (median) and 90% power spectra percentiles are about 7 dB higher in the 437 MHz band as compared to the 435 MHz band, but not the 10% percentile that is 4 dB lower. A band-limited signal appears in all cases and is in the centre of the band, except for the 10% percentile at 437.28 MHz. In fig. 2a the bandwidth of this signal is 300 kHz and in the 50% and 90% percentile of fig. 2b the bandwidth is 200 kHz. The 300 kHz interference signal appears in all the percentiles of the 435 MHz measurements.

The coefficient of variation, which measures the spread in the average envelope, is also higher for the 437.28 MHz case. Within the SDR bandwidth marked by the vertical black dotted lines, the CV is higher where the band-limited interference signal can be seen in the average power spectra plots. High power and high CV indicate that there are strong signals with a high spread in magnitude. A high CV is often the result of repeated short bursts of high power [20]. Figure 2c also shows that the signals measured do not follow a Additive White Gaussian Noise (AWGN) behaviour. Thus, applying countermeasures and estimating link budgets assuming AWGN will not be useful in this environment.

The time variability of the north to south passes in Europe and the high north has been analysed in fig. 3.

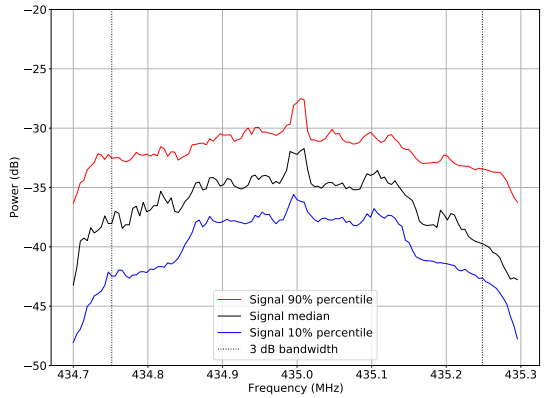

(a) Average power spectra percentiles centered at 435 MHz.

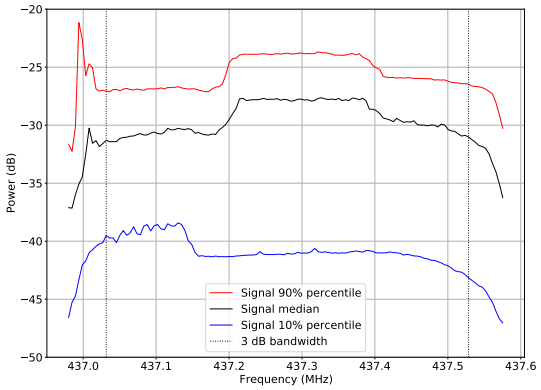

(b) Average power spectra percentiles centered at 437.28 MHz.

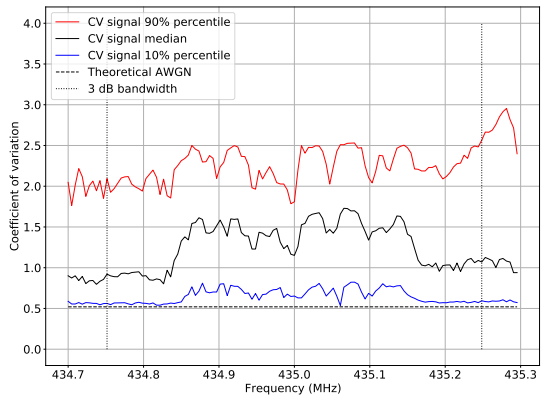

(c) Coefficient of variation percentiles centered at 435 MHz.

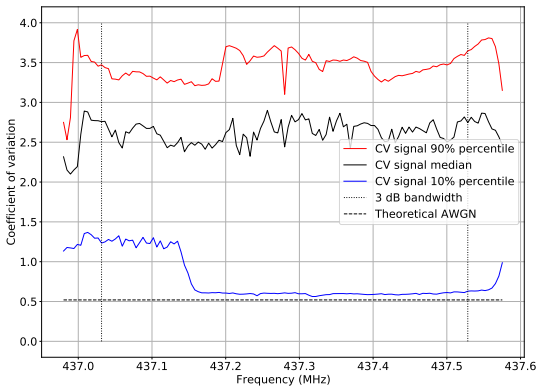

(d) Coefficient of variation percentiles centered at 437.28 MHz.

Fig. 2. Time and frequency statistics. A high spread in the average envelope corresponds to a high CV.

The average power spectra has been integrated over the 500 kHz bandwidth and plotted against time. The measurement tracks are from north to south and the time between measurement points is one minute. The variation of the integrated power over the bandwidth for the northern passes is shown in fig. 3c. The power values of the different measurements follow a similar trend, increasing 12 dB as the satellite moves from north to south. The power levels measured over the high north are similar to the levels in the southern part of the tracks in fig. 3d.

In fig. 3d, all the tracks over western Europe show a similar tendency in integrated power. The values of the red and blue passes over western Europe are more similar since they are closer to each other. As the tracks move to the east, the power drop is delayed. There is higher power when the satellite is over central Europe.

To get an overview of the spatial power variation, the measurements points at 437.28 MHz in fig. 1 that are between -35° to 35° in longitude have been divided into regions in fig. 4a, similarly to [19]. The Empirical Cumulative Density Functions (ECDFs) of average power during each 5 s measurement including all frequency bins within the bandwidth are shown in fig. 4b. The colours of the measurement points in the map correspond to those in the ECDFs. About 80% of the measurement points over 75° latitude and those in the south-west corner have power levels 13 dB lower than in central Europe. The region between 60° – 75° has about 5 dB less power than central Europe for 80% of the points. These results explain the difficulties experienced by small satellite operators from universities located in central Europe, including UVigo (Spain). This university is located in the north-west of Spain where the interference power behaviour changes from region $R1$ to $R2$.

The window of stationarity of first-order was estimated using the LME method and the CV for each time window as described in [19]. In fig. 5, the time variability of the measurements centered at 435 MHz and the ones

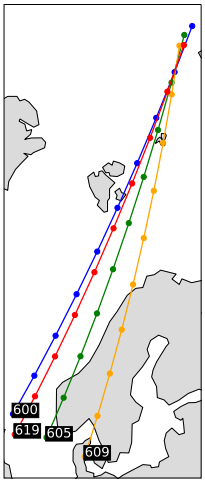

(a) Measurement passes over the high north and Scandinavia.

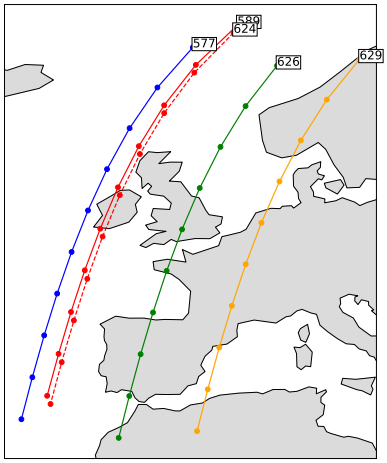

(b) Measurement passes in the west of Europe.

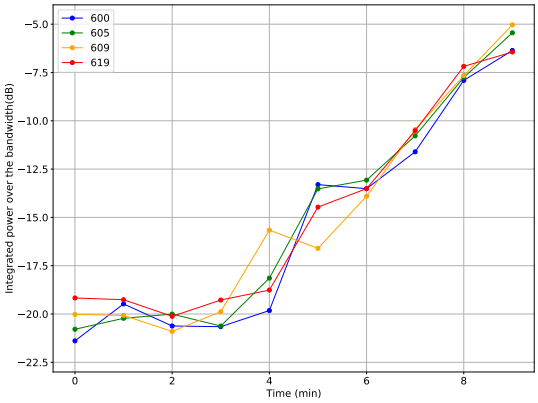

(c) Integrated power over bandwidth for passes over the high north and Scandinavia.

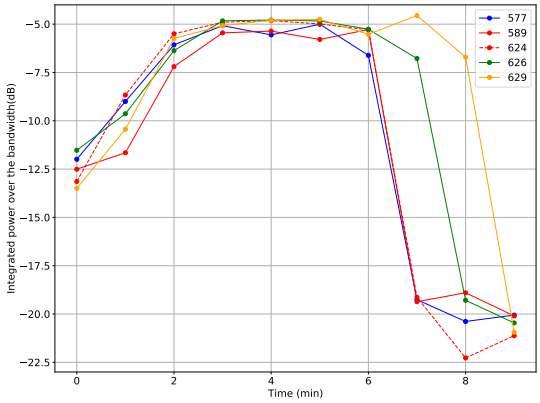

(d) Integrated power over the bandwidth for passes in the west of Europe.

Fig. 3. Integrated power over bandwidth for north-south passes in Europe and the high north centered at 437.28 MHz.

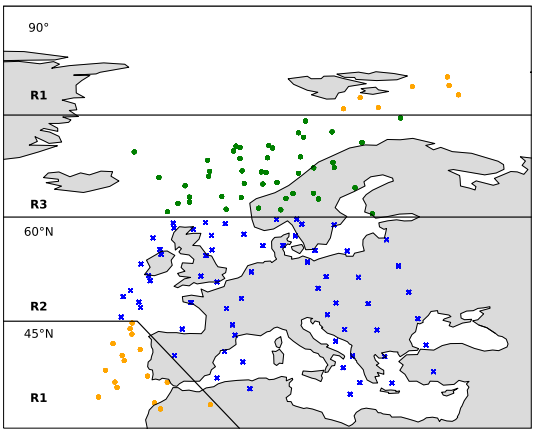

(a) Measurement positions divided into three regions.

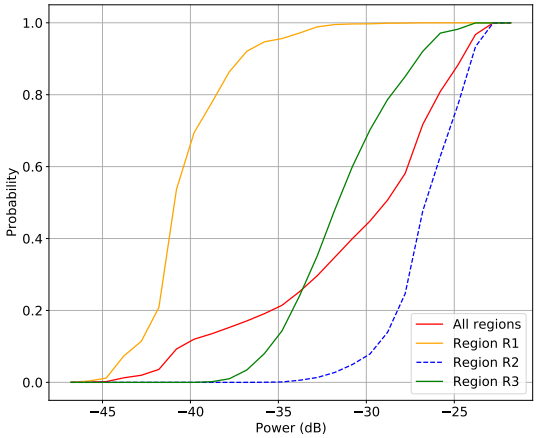

(b) Empirical Cumulative Density Function (ECDF) of average power over the three regions. All frequency bins have been included in the estimation.

Fig. 4. Distribution of average power over over Europe and the high north.

at 437.28 MHz is compared both within the band-limited signal bandwidth and outside. For the 435 MHz case, the bandwidth was 300 kHz, and for the 437.28 MHz, 200 kHz. The percentage of measurements with a stationarity window longer than 27.3 ms is higher for the new measurements at 437.28 MHz both within the bandwidth of the band-limited signal (solid filled bars) and outside (patterned bars). It is almost 70% compared to the 43% (within) and 30% (outside) of the 435 MHz measurements. These results indicate that the interference has a high time variability and most measurements do not show a stationary behaviour in windows shorter than 27.3 ms. Thus, to be able to estimate interference statistics the time window to be used should be at least longer than 30 ms because there is too much time variability in lower time scales.

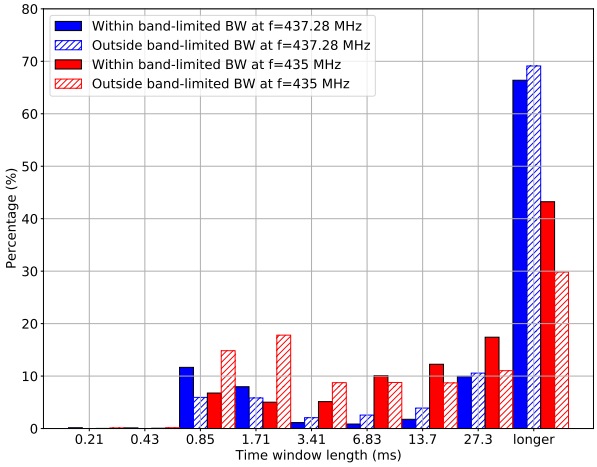

Fig. 5. Stationarity window histogram comparing the measurements centered at 435 MHz and 437.28 MHz.

4. Conclusions

We have presented time and frequency measurement results of in-orbit radio interference from the LUME-1 satellite. This article showed the results of 150 individual 500 kHz bandwidth measurements in the 437 MHz band over Europe comparing them to the 435 MHz band, also within the UHF amateur band.

The average interference power and the spread in envelope was higher in the 437.28 MHz band than in the 435 MHz band, explaining challenges experienced by operators of small satellites. A 200 kHz band-limited interference signal was detected in the new measurements centered at 437.28 MHz in contrast with the 300 kHz bandwidth of the signal at 435 MHz. The interference behaviour is highly non-Gaussian, so countermeasures, such as error correction codes, and link budgets that assume AWGN will not be realistic in this band.

Building interference statistics require many measurements to gather the long-term time variability. These statistics can be useful in designing or improving existing satellite communication systems.

Acknowledgements

The work of Norwegian University of Science and Technology (NTNU) is supported by the Norwegian Research Council (Grant No. 270959), the Norwegian Space Agency, and the Centre of Autonomous Marine Operations and Systems (NTNU AMOS). The work of UVigo is supported by Ministerio de Ciencia e Innovación in Spain (Grant No. ESP2016-79184-R).

References

[1] ITU-R: Report ITU-R SA.2312-0. *Characteristics, definitions and spectrum requirements of nanosatellites and picosatellites, as well as systems composed of such satellites*. Tech. rep. ITU, 2014.

[2] ITU-R: Report ITU-R SA.2348-0. *Current practice and procedures for notifying space networks currently applicable to nanosatellites and picosatellites*. Tech. rep. ITU, 2015.

[3] Fernando Aguado Agelet, Diego Nodar López, and Alberto González Muiño. "Preliminary noise measurements campaign carried out by HUMSAT-D during 2014". In: *ITU Conference and Workshop on the Small Satellite Regulation and Communication Systems*. Mar. 2015, pp. 1–21.

[4] S. Busch et al. "UWE-3, in-orbit performance and lessons learned of a modular and flexible satellite bus for future pico-satellites". In: *Acta Astronautica* 117 (2015), pp. 73–89. ISSN: 0094-5765. DOI: 10.1016/j.actaastro.2015.08.002. URL: http://dx.doi.org/10.1016/j.actaastro.2015.08.002.

[5] Gara Quintana-Diaz et al. "Detection of radio interference in the UHF amateur radio band with the Serpens satellite". In: *Advances in Space Research* 69.2 (2022), pp. 1159–1169. ISSN: 0273-1177. DOI: https://doi.org/10.1016/j.asr.2021.10.017. URL: https://www.sciencedirect.com/science/article/pii/S0273117721007778.

[6] Martin Buscher. *Investigations on the current and future use of radio frequency allocations for small satellite operations*. Vol. 7. Universitätsverlag der TU Berlin, 2019. ISBN: 9783798330726.

[7] European Space Agency (ESA). *ESA Artes frequency monitoring*. https://artes.esa.int/projects/board-spectrum-monitoring-obsm. 2016.

[8] European Space Agency. *On-board Interference Geo-location System (ARTES 5.1 5A.037)*. https://artes.esa.int/funding/onboard-interference-geolocation-system-artes-51-5a037-0. 2016.

[9] European Space Agency (ESA). *Spectrum Monitoring Mission Feasibility Assessment(ARTES FPE 1B.129)*. https://artes.esa.int/funding/spectrum-monitoring-mission-feasibility-assessment-artes-fpe-1b129. 2016.

[10] European Space Agency. *Radio Frequency Analytics Applications (ARTES)*. https://business.esa.int/funding/call-for-proposals-artes-satcom-apps/radio-frequency-analytics-applications. 2021.

[11] Aurora Insight Inc. *Aurora Insight*. https://aurorainsight.com/.

[12] *Iluminate the world | Umbra*. https://umbra.space/. Accessed on 22/12/2021.

[13] K. Sarda et al. "Making the Invisible Visible: Precision RF-Emitter Geolocation from Space by the HawkEye 360 Pathfinder Mission". In: *Proceedings of the 32nd Annual AIAA/USU Conference on Small Satellites*. "Logan UT, USA", 2018.

[14] *Space Powered Signal & Geospatial Intelligence | Kleos*. https://kleos.space/. Accessed on 22/12/2021.

[15] *Amber Space-Based Maritime Domain Intelligence Solutions | Horizon Technologies*. https://horizontechnologies.eu/products/cubesat/. Accessed on 22/12/2021.

[16] *University of Vigo- LUME-1 satellite. Telemetry modulation, codes and format*. http://fire-rs.com/static/pdf/LUME-TMandBeacons-1.4-20190107_4.pdf. University of Vigo.

[17] *Orbit NTNU- Selfie Sat*. https://orbitntnu.com/selfiesat/. Orbit NTNU.

[18] Franco Pérez-Lissi et al. "FIRE-RS: Integrating land sensors, cubesat communications, unmanned aerial vehicles and a situation assessment software for wildland fire characterization and mapping". In: *69th International Astronautical Congress*. 2018.

[19] Gara Quintana-Diaz et al. "In-Orbit Measurements and Analysis of Radio Interference in the UHF Amateur Radio Band from the LUME-1 Satellite". In: *Remote Sensing* 13.16 (2021). ISSN: 2072-4292. DOI: 10.3390/rs13163252. URL: https://www.mdpi.com/2072-4292/13/16/3252.

[20] Gara Quintana-Díaz et al. "In-orbit Interference Measurements and Analysis in the VDES-band with the NorSat-2 Satellite". In: *2022 IEEE Aerospace Conference (AERO)*. 2022, pp. 1–8. DOI: 10.1109/AERO53065.2022.9843810.